Nitzschia captiva sp. nov. (Bacillariophyta), the essential prey diatom of the kleptoplastic dinoflagellate *Durinskia capensis*, compared with *N. agnita*, *N. kuetzingioides* and other species

DAVID G. MANN[1,2], NORICO YAMADA[3], JOHN J. BOLTON[4], ANDRZEJ WITKOWSKI[5] AND ROSA TROBAJO[2]

[1]*Royal Botanic Garden Edinburgh, Edinburgh EH3 5LR, Scotland, UK*

[2]*Marine and Continental Waters, Institute for Food and Agricultural Research and Technology (IRTA), Crta de Poble Nou Km 5.5, E-43540 La Ràpita, Catalunya, Spain*

[3]*Department of Biology, University of Konstanz, Universitäts str. 10, Konstanz, Baden-Württemberg, Germany*

[4]*Department of Biological Sciences, University of Cape Town, South Africa*

[5]*Institute of Marine and Environmental Sciences, University of Szczecin, Mickiewicza 16 str., 70-383 Szczecin, Poland*

CONTACT

Corresponding author: David Mann; E-mail: dmann@rbge.org.uk

ACKNOWLEDGEMENTS

We are very grateful to Dr Lena Eggers for finding and sending type material of *N. agnita* and *N. kuetzingioides* from the Hustedt Collection (Alfred Wegener Institute, Bremerhaven, Germany); the late Dr Luc Ector for help with diatom literature; Frieda Christie, Ruth Hollands and Dr Kanae Nishii for support of the SEM and LM facilities at the Royal Botanic Garden Edinburgh; Sam Bolton for technical assistance; and two anonymous reviewers for constructive comments.

FUNDING

Initial support for our work was provided by the project ‘Biodiversity and evolution of algae in the Indo-Pacific: a Japan/South Africa comparison’ (Strategic International Research Cooperative Program to J.J. Bolton) of JST in Japan and NRF in South Africa. The establishment of the *N. captiva* strain was then financially supported by a Bridging Stipend of University of Konstanz (No.638/20, to N. Yamada), and a DFG Research Grant (No. YA 577/2-1, to N. Yamada). We also acknowledge support from the CERCA Programme, Generalitat de Catalunya. The Royal Botanic Garden Edinburgh is supported by the Scottish Government's Rural and Environment Science and Analytical Services Division.

RUNNING TITLE

Nitzschia captiva, the kleptoplastid of *Durinskia capensis*

ABSTRACT

Durinskia capensis is a kleptoplastic dinoflagellate species from high intertidal marine rock pools, which can use a variety of diatoms for photosynthesis. However, very few of the diatoms permit indefinite survival of the dinoflagellate and *rbc*L sequences show that *D. capensis* isolated from nature contains one of two closely related *Nitzschia* species as its kleptoplastids. In culture, without a supply of these 'essential' *Nitzschia* cells to replenish the intracellular store of diatom plastids and other organelles, *D. capensis* eventually loses all its kleptoplastids and dies. Inside *Durinskia*, diatoms do not possess frustules and so cannot be compared morphologically with free-living forms. Recently, one of the essential *Nitzschia* species was isolated from the type locality of *D. capensis* and grown in culture, allowing comparison with similar *Nitzschia* species, particularly *N. agnita* and *N. kuetzingioides*, examined from type material. We conclude that the 'essential diatom' of *D. capensis* differs morphologically from these and other *Nitzschia* species and it is therefore described as *N. captiva sp. nov. Nitzschia agnita* and *N. kuetzingioides*, on the other hand, are conspecific and *N. agnita* has priority. *Nitzschia captiva* and *N. agnita* are extremely similar in valve shape, dimensions, pattern and ultrastructure, but can be separated by their girdle structure. *Nitzschia agnita* appears to be a freshwater species, though somewhat salt-tolerant. In contrast, *N. captiva*, which is known principally from records of the kleptoplastids of *D. capensis* rather than from frustules, is so far marine.

KEYWORDS

Dinotom; Dinoflagellates; Endosymbionts; Kleptoplastids; Taxonomy

INTRODUCTION

It has been known since the 1970s that some dinoflagellates contain chloroplasts that contain fucoxanthin as the principal accessory carotenoid pigment, instead of the more usual peridinin (Riley & Wilson 1967; Mandelli 1968) and chlorophylls c_1 and c_2 (Withers & Haxo 1975). These dinoflagellates were also found to be unusual in that their chloroplasts are located within a cellular compartment containing its own nucleus with ribosomes and mitochondria, which is separated from the remainder of the dinoflagellate cell by a single membrane (e.g. Tomas & Cox 1973; Tomas *et al.* 1973). The extra nucleus does not have the 'mesokaryotic' structure typical of dinoflagellates, with condensed chromosomes, but has an appearance more like that of the majority of eukaryote nuclei, with dispersed chromatin (e.g. Dodge 1971; Tomas *et al.* 1973). Almost from the outset it was realized that the second nucleus, the unusual chloroplasts (with their anomalous pigment composition) and the other organelles associated with them, represented an endosymbiont, though its affinities were initially unclear: Withers & Haxo (1975) suggested that the endosymbiont of *Peridinium foliaceum* (F. Stein) Biecheler (currently *Kryptoperidinium triquetrum*; see Gottschling *et al.* 2019) had an "affinity with the brown algae, chrysomonads, or diatoms". Once DNA sequence data became available, however, it became possible to determine the identities of the fucoxanthin-containing endosymbionts and show that many of them are diatoms (e.g. Chesnick *et al.* 1996), which exist within the dinoflagellate cells as naked protoplasts, lacking frustules. The endosymbionts belong to the three families of diatoms: Bacillariaceae, Stephanodiscaceae and Chaetocerotaceae (Yamada *et al.* 2017), while all of the diatom-containing dinoflagellates belong to the single family Kryptoperidiniaceae (Gottschling *et al.* 2017).

Recently, it has been found that in one of the diatom-containing dinoflagellates (also called dinotoms), *Durinskia capensis* Pienaar, H. Sakai & T. Horiguchi, the diatoms are not

permanent inhabitants of the cells. Unlike its close relatives, such as *D. kwazulunatalensis* Norico Yamada, Sym & T. Horiguchi (Yamada *et al.* 2017) and *D. oculata* (F. Stein) Gert Hansen & Flaim (Kretschmann *et al.* 2018), which have permanent endosymbionts, *D. capensis* has to keep replenishing its diatoms by new acquisitions from the environment – it is kleptoplastic (Yamada *et al.* 2019) – and if it is starved of suitable prey for nine weeks (as a maximum), the cells become colourless and finally die. Moreover, feeding trials and sequencing of cells from nature show that *D. capensis* is very selective (Yamada *et al.*, unpublished). Although it can feed on many different diatoms and derive some benefit from them, only one or two species are able to sustain it indefinitely through their photosynthesis. These 'essential' diatoms have been identified as *Nitzschia* species by their *rbc*L sequences (Yamada *et al.* 2017, 2019; Mann *et al.* 2021a), since inside the *Durinskia* they lack frustules, preventing comparisons based on morphology. In 2018, we isolated one of these 'essential' diatoms, making it possible for the first time to maintain *D. capensis* in stable culture (Yamada *et al.* 2019). The purpose of the present paper is to establish the identity and relationships of this diatom, which has until now been referred to as '*Nitzschia* cf. *agnita*' (Yamada *et al.* 2019). To do this we also studied the type material of *N. agnita* Hustedt and *N. kuetzingioides* Hustedt. It should be noted that the *D. capensis* '*Nitzschia* cf. *agnita*' is not the same diatom as the '*Nitzschia* cf. *agnita*' studied by Lundholm *et al.* (2002).

MATERIAL AND METHODS

Durinskia capensis is a marine species, which has been collected from several sites in the Western Cape Province (Lamberts Bay, Saldanha Bay and Kommetjie; Pienaar *et al.* 2007; Yamada *et al.* 2017), South Africa, where it occurs in tidal pools high on the shore. In October 2018 samples of biofilm and water were collected by JJB from the tidal pools at Kommetjie from which *D. capensis* was originally described by Pienaar *et al.* (2007). From

these a number of diatom species were isolated by RT (Yamada *et al.* 2019), including a *Nitzschia* species that corresponded to one of the known *rbc*L haplotypes of *D. capensis*. This isolate, IRTA-CC-152, identified as '*N.* cf. *agnita*', has subsequently been maintained in unialgal culture and used for co-culture with isolates of *D. capensis* (Yamada *et al.* 2019). Cultures were grown in f/2 medium with silicate with a 12:12 h dark:light photoperiod. We grew stock cultures at 10°C to help reduce the frequency of transfer to new medium and these provided cells of approximately the same length as type material of the other two species considered in detail here (*N. agnita* and *N. kuetzingioides*). Over time, cell length decreased in culture and was then restored apparently without pairing (the details of the process have yet to be established), so that there is every prospect that cultures can be kept indefinitely.

To investigate the possible effects of temperature and life cycle progression on the morphology of *N.* cf. *agnita,* we also studied specimens from lineages derived from the original IRTA-CC-152 isolate and grown at 16 or 20°C for at least one year. As a result of the more rapid growth at higher temperatures, these lineages differed in the mean lengths of the cells, the 20°C lineage now existing as very small cells of 8 μm or less and the 16°C lineage as cells 14–20 μm long. Since cells of this species change in their physiological and molecular biological profiles in the days after subculturing (Yamada *et al.*, unpublished), we checked for accompanying morphological changes by inoculating the 20°C and 16°C cultures into new medium 15 and 6 days before harvesting (giving lineages 20-A, 20-B, 16-A and 16-B). In addition, we examined seven-months-cryopreserved material of an axenic culture that had been grown at 20°C before preservation. This had cells of intermediate length, 9–12.5 μm long (Table S1). None of these temperatures (10, 16 and 20°C) are unrealistic for the natural habitat from which IRTA-CC-152 was obtained (see below, 'Ecology and geographical distribution').

Cleaned frustules of IRTA-CC-152 were prepared either by heating with concentrated nitric and sulphuric acids (followed by washing with deionized water), or by the rapid cleaning method described by Trobajo & Mann (2019). For preparation of permanent slides, coverslips with dried-down material were mounted on glass slides using Naphrax (refractive index 1.74; Brunel Microscopes: http://www.brunelmicroscopes.co.uk/). Voucher slides and material of IRTA-CC-152 have been incorporated into the diatom herbarium at the Royal Botanic Garden Edinburgh (RBGE, herbarium abbreviation E) as E5899 and further slides are deposited in the diatom collection of IRTA. Aliquots of type material of *Nitzschia agnita* (sample 10096) and *N. kuetzingioides* (sample E8145) were obtained from the Hustedt collection (Alfred Wegener Institut, Bremerhaven, Germany) and prepared for light- and scanning electron microscopy by the rapid cleaning method. The microscope slide preparations used are listed in Table 1.

Light microscopy (LM) was performed using either a Nikon Eclipse 90i photomicroscope or a Zeiss Axio Imager photomicroscope, in both cases with Plan-Apochromat 100× objectives (N.A. 1.4) and differential interference contrast (Nomarski) optics. Photographs were taken with a DS-Ri1 (Nikon Eclipse) or an AxioCam HRc camera (Zeiss Axio Imager). For scanning electron microscopy (SEM), material was dried onto small cover-slips (13-mm diameter), which were then attached to stubs using carbon discs and electrical conduction improved by application of silver dag paint (Electrodag 1415, Agar Scientific, Stansted, UK) and sputtered with platinum for 1–2 min in an Emitech K575X sputter coater. Stubs were examined using a LEO Supra 55VP Field Emission SEM operated at 5 kV (*c.* 4 mm working distance; aperture 20 μm), at zero or 25° tilt.

Stria and fibula densities were determined parallel to the apical axis, over 5 or 10 μm, respectively. Poroid spacings were determined by using Adobe Photoshop to define and extract a rectangular area in SEM photographs of valve interiors at zero tilt, within which a

random selection of poroids was identified and the distance measured of each poroid to its immediate neighbour within the same stria (always the poroid on the right-hand side as viewed). For this, all images were adjusted to the same magnification and the same size of rectangular area defined in each (3.70 µm × 2.13 µm, the latter being chosen so that the rectangle would fit within the width of the valve in all cases). Photoshop was also used to make general adjustments to photographs using the Brightness/Contrast, Levels and Curves tools, and, in the case of LM images of valves captured in colour, by choosing the Black and White filters that gave the best compromise between enhanced resolution and the visually most attractive representation of the fibulae.

Discovery of 'short bands' like those present in *N.* cf. *agnita* was reported by Mann *et al.* (2021b), where their nature and distribution was discussed. Otherwise, frustule terminology follows von Stosch (1975) Ross *et al.* (1979) and Round *et al.* (1990).

A phylogenetic tree of '*N.* cf. *agnita*', *Durinskia capensis* and other Bacillariaceae was prepared using all unique *rbc*L sequences of Bacillariaceae available in May 2022: we took the trimmed alignment used by Mann *et al.* (2021a), excluding the *Craspedostauros–Achnanthes–Staurotropis* group, and added new accessions from GenBank. The alignment was partitioned by codon position and analysed using raxmlGUI 2.0 (Edler *et al.* 2021), with a GTR+gamma model and 1,000 bootstrap replicates. The resulting tree was visualized and prepared for publication using iTOL v5 (Letunic & Bork 2021). For clarity, we collapsed most major clades of Bacillariaceae apart from the one (Clade 6B of Mann *et al.* 2021a) containing the target species.

RESULTS

'*Nitzschia* cf. *agnita*' IRTA-CC-152

So far, this diatom is known only from cultures of isolate IRTA-CC-152, established in 2018, and from records of it as the kleptoplastids of *Durinskia capensis*. Its *rbc*L sequence (NCBI accession LC482715) places it in Bacillariaceae Clade 6B in the phylogeny of Mann *et al.* (2021a; Fig. 1). Samples collected for metabarcoding in 2020 from the Kommetjie pools were examined morphologically (by AW) but did not reveal valves of the species, either in SEM or LM, even though the metabarcoding data (using an *rbc*L marker: manuscript in preparation) have since shown that it was present: virtually all of the DNA reads must have come from *N.* cf. *agnita* living within the abundant *D. capensis* present. Consequently, the description that follows is based only on samples from cultures, where *N.* cf. *agnita* grows well. After more than three years in culture, cells of IRTA-CC-152 appear as vigorous and healthy as they did initially, responding quickly to transfers to new medium. They are quite variable in shape and size and the frustules are delicate. Their morphological characteristics are as follows:

Valves are linear-lanceolate to lanceolate or even elliptical in the smallest valves, 5.5–29 µm long and 3.3–4.8 µm wide, with 13.7–16.8 fibulae in 10 µm (Table 1; Figs 2–6, 13–16, 23–25, S1–S3); valves are very finely structured and delicate and it was impossible to resolve the striae in LM. There are two chloroplasts per cell, placed fore-and-aft in the cell (Figs 13–19), each containing a single pyrenoid (Fig. 13, arrow). There are usually two small volutin granules per cell, just beyond the ends of the chloroplasts (Fig. 19, arrow). None of these cytological characters is unusual for Bacillariaceae (Mann 1978; Mann *et al.* 2021a). The depth of the cell is *c.* 3 µm at the beginning of interphase (Fig. 17), increasing to *c.* 4 µm before cell division (Figs 18, 19) and closer to 4.5 µm during division (Figs 20, 21). The

small size of the cells made it impossible to determine whether the chloroplasts divide before or during cytokinesis (cf. Geitler 1975; Round *et al.* 1990, fig. 51(B)a).

The valve outline is variable, some valves showing a more-or-less smoothly changing curvature from centre to poles (e.g. Figs 4, 13) while others are parallel-sided at the centre (Figs 2, 3, 14). Longer specimens generally have narrow, attenuate, rostrate (Figs 2–5) or subcapitate ends (Figs 24, 30), which are lost as size reduction occurs during the life cycle, so that the valve shape becomes simpler and lanceolate, with acute apices (Figs S2, S3). However, some specimens have broader, more rounded ends (Fig. 6), and short specimens can have bluntly rounded ends (Figs S2, S3), especially when alive (Fig. 16). Distorted frustules became common in older cultures (e.g. Figs 22, S3). The raphe system runs along one margin of the valve and is subtended by small fibulae that appear as dots in LM (Figs 2–6). The two central fibulae are not more widely spaced than the others (Figs S1, S2).

SEM revealed a simple valve structure with dense uniseriate striae: there are 50–52 striae in 10 µm in valves 25–30 µm long (i.e. in valves that are approximately the same length as the other two species being compared here) (n = 5). They contain extremely small round poroids (Figs 23–25, 30, 32, 35). The valve face inclines gently from the raphe canal outwards to the distal mantle, which is extremely narrow and delicate (Figs 37, 38, 40). Indeed, the distal mantle often collapses completely (Fig. 35). The poroids are generally more or less evenly spaced along the striae, *c.* 41.7–51.5 in 10 µm (the 5 valves measured had average spacings of 41.7, 41.8, 44.5, 47.2, 50.0 and 51.5 in 10 µm, for n = 27, 25, 29, 32 and 35 measurements, respectively). The valves are lightly silicified and in many specimens the poroids appeared empty, both internally and externally (Figs 30, 40). However, in some specimens (presumably the better preserved ones), the poroids could be seen to contain hymenes, positioned closer to the external apertures of the poroids (Figs 38, 46, 49); this was especially evident in the poroids of the raphe canal (Fig. 38). Within the raphe canal, each

transapical stria is represented by a single poroid (Figs 30, 38, 40, 49), with a slight separation between this and the remainder of the poroids in the stria.

The raphe is continuous across the centre of the valve (Figs 38, 40) and the external slit is apparently unaccompanied by ridges or flanges (an example of a *Nitzschia* species with such ridges is given by Mann *et al.* 2021a, fig. 2A). The terminal fissures are short and bent to one side (either towards or away from the mantle: see Figs 30 and 40, respectively). The fibulae are mostly small and stubby (Figs 23, 24) but can also be more rib-like (Figs 25, 32); in the early stages of valve formation all of the fibulae are narrow and rib-like (Fig. 45). In mature valves, the fibula bases are expanded and connected by a narrow longitudinal rib (Figs 32, 35), which corresponds to the wider separation of the stria poroids already noted at the base of the raphe canal (compare Figs 35 and 38).

A key feature of *N.* cf. *agnita*, relative to the other two species considered in detail here, is the structure of the girdle, which has been described briefly by Mann *et al.* (2021b). Instead of being composed wholly of open bands that extend from pole to pole, as in most Bacillariaceae (e.g. Mann *et al.* 2021a), four out of the five bands present in the cingulum (bands 1 to 4) are short, extending from close to the centre of the cell on one side around the pole to close to the centre of the cell on the other side (Figs 43–46). Hence, views of the centre of a theca show the opposed ends of four girdle bands, with band 2 opposed to band 1 and band 4 opposed to band 3 (Figs 45, 46). The ends of the bands taper unequally, making it possible to determine which band is which even when they are separated from the valve. In bands 1 and 3, the advalvar margin is more or less straight throughout, whereas the abvalvar margin is curved towards the ends of the bands (Fig. 47). In bands 2 and 4, it is the abvalvar margin that is straight (e.g. band 4 in Fig. 48). The only band that extends from pole to pole is band 5 (the band furthest from the valve), which is open at one pole and continuous at the other (Fig. 48). Bands 1 and 2 are wider and coarser than bands 3 and 4 but all bear two rows

of slightly elongate poroids. Band 5 bears only one row of poroids and is extremely narrow and delicate (Figs 47, 48). Because of this, band 5 is insufficiently strong to maintain the integrity and shape of the girdle when the cells are treated to remove the organic content. Consequently, when thecae begin to disassemble after cleaning, the four wider bands splay apart and demonstrate their short length relative to the valves. This is easily detected in LM (Figs 41, 42), as well as in SEM (Fig. 43). In many tens of examples observed with LM or SEM, none were found in which the girdle retained the shape of the cell after detachment from the valve.

No differences in valve or girdle structure were observed between valves from 10, 16 and 20°C cultures (Fig. S3), except for a higher incidence of deformed frustules in the two 20°C cultures with extremely small cells (a well-known phenomenon in pennate diatoms: cf. Geitler 1932). Stria densities were higher in the 16 and 20°C cultures than in the 10°C material (*c.* 53 in 10 μm rather than *c.* 50; Table S1), but since there were no consistent differences between stria densities in the 16 and 20°C valves it seems quite likely that the lower stria densities in the 10°C material were associated with the much greater valve length (i.e. stage in the life cycle), rather than with temperature *per se*. As far as we know, no-one has detected an experimental effect of temperature on stria density in pennate diatoms (e.g. see Mizuno 1987), whereas a correlation between higher stria density and shorter valves has been seen in clonal material of *Nitzschia fonticola* (Grunow) Grunow (Trobajo *et al.* 2006) and has been noted more generally in pennate diatoms (Geitler 1932, p. 186, ‘ad. 4’). There were no consistent differences in stria density or frustule morphology between cells inoculated into new medium 6 and 10 days before harvesting (Table S1).

Nitzschia agnita Hustedt (1957, p. 347, fig. 51)

LECTOTYPE: marked, unnamed specimen on Hustedt Collection slide 385/98 (a preparation of cleaned material from a mixed natural population), 'Bremen. Ochtum. 7' (selected and illustrated by: Lange-Bertalot & Simonsen 1978, p. 16, fig. 151; Simonsen 1987, p. 444, pl. 661, figs 5, 6).

TYPE MATERIAL: Hustedt Collection, sample 10096: the 'Ochtum 7' sample was collected on 20 November 1956 from bottom mud in the River Ochtum (a tributary of the Weser), somewhat above a sewage inflow at Kattenesch, Germany, where it forms the border between Lower Saxony and Bremen.

ETYMOLOGY: *agnitus* means 'discerned' or 'recognized'; given that Hustedt may only have seen one specimen and that this had very delicate (unrecognizable!) structure, the name may perhaps have been a joke.

As shown by our use of the name '*Nitzschia* cf. *agnita*', the diatom most similar to IRTA-CC-152 in the classic account of *Nitzschia* by Krammer & Lange-Bertalot (1988) is *N. agnita*, because of its shape, size and delicate structure. Hustedt (1957) described *N. agnita* from the river Ochtum at Kattenesch, near Bremen, N Germany. The original description gave the valve outline as lanceolate with convex sides, about 33 µm long and 3.5 µm wide, with some 18 very small fibulae in 10 µm: Hustedt emphasized the shape of the valve ends – very narrowly rostrate, with capitate apices ("sehr schmal geschnäbelten, an den Polen kopfig gerundeten Enden") – as particularly important in separating *N. agnita* from similar small-celled species. As noted by Archibald (1983, p. 233), the fact that Hustedt gave a single measurement for the length and breadth of *N. agnita* suggests that he may only have observed one specimen. If so, it would probably be the marked specimen (a frustule) found and illustrated by Lange-Bertalot & Simonsen (1978) and Simonsen (1987). However, since this specimen was not specifically named, either on the slide or in Hustedt's (1957) paper, its identification as the 'holotype' cannot be conclusively established, especially because the fibula density in this specimen does not match that given by Hustedt (Table 1). We therefore regard Lange-Bertalot & Simonsen and Simonsen as having designated a lectotype, which is

the marked specimen at Carl Zeiss Finder reference 282.9 (for the Finder specification, see Simonsen 1987, p. 5) on Hustedt Collection slide 385/98 ‘Bremen. Ochtum. 7’.

During our examination of the same material from which the type slide was made (Hustedt Collection, sample 10096), we found just two specimens that could be assigned to *N. agnita* after searching three LM slides and one stub, confirming the rarity implied by Hustedt’s description and suggested by Archibald (1983). In LM we observed two frustules, one shown here in two focuses (Figs 7, 55), the second in Fig. S3; in SEM we found a single valve in internal view (Fig. 26). These three specimens, together with measurements from photographs of the single *N. agnita* found by Lange-Bertalot & Simonsen (1978) and Simonsen (1987, pl. 661, fig 5, 6), provide the basis for a strict circumscription of *N. agnita*, based only on type material, with which other material and species can be compared (Table 1).

The valves are narrowly lanceolate, with a smoothly changing curvature in the central part of the valve (which therefore lacks a linear section). The ends of the valves are drawn-out in the two longer specimens but not in the shortest one (Fig. 26); all have very narrow, distinctly capitate apices (Figs 7, S3; Simonsen 1987, pl. 661, figs 5, 6). The dimensions are: length 23–35 µm, width 3.3–3.7 µm, with 14.8–15.6 fibulae in 10 µm; the original description gave *c.* 18 fibulae in 10 µm but we could not replicate this measurement from the lectotype as illustrated by Simonsen (1987; see Table 1, footnote 2). The central fibulae are not more widely separated (this was noted also by Hustedt 1957) and there is no central nodule. The striae are invisible in LM with N.A. 1.4 lenses and an oiled condenser. SEM revealed (1 measurement) a stria density of 51 in 10 µm (Fig. 26).

The valve ultrastructure agrees in all respects with that of *N.* cf. *agnita*, except that the stria poroids were more irregularly and more widely spaced in the single specimen found (Figs 26, 33, contrast Figs 23–25, 32): the poroid spacing along the striae averaged 37.6 in 10

µm (*n* = 30). The central part of the raphe was obscured by debris (Fig. 26), so we were unable to confirm directly that the raphe slit is continuous.

The single specimen found in SEM lacked any associated girdle bands and so no details of girdle structure were observed. However, the two LM specimens we found, and also the lectotype illustrated by Simonsen (1987), were all frustules and in one of them the girdle had partly collapsed inwards, part of it appearing as a single continuous line crossing the interior space obliquely (Fig. 52). There was no break or abrupt bend in this line and so we consider that short bands, like those in all frustules of *N.* cf. *agnita* (Figs 41–51), were absent. There was also no sign of short bands in the two other frustules that have been observed (one in Fig. S4, the other shown by Simonsen 1987, pl. 661, figs 5, 6), but this may be because they were still more or less intact despite treatment with oxidizing acids (in the case of the frustule shown in Fig. S4, there had been two treatments, one by Hustedt and one by us to remove organic preservatives). This may be significant, because our experience with *N.* cf. *agnita* is that even one treatment in this species (with the rapid cleaning method) is usually sufficient to release the short bands.

Nitzschia kuetzingioides Hustedt *ex* Lange-Bertalot & Simonsen (1978, p. 38, figs 152–154)

ORIGINAL DESCRIPTION (invalid): Hustedt (1959), p. 417, figs 25–29

VALIDATING DESCRIPTION: Lange-Bertalot & Simonsen (1978, p. 38, figs 152–154)

HOLOTYPE: Hustedt Collection, slide 327/19b (a preparation of cleaned material from a mixed natural population).

TYPE MATERIAL: Hustedt Collection, sample E8145, obtained from bottom mud (“Grundschlamm”) collected on 25 May 1950 at Neusiedl (at the N end of the Neusiedler See) by Dr E. Peschek under 0.5 m water (information collated from Hustedt 1959 and Simonsen 1987).

ETYMOLOGY: the name indicates a resemblance to *N. kuetzingiana* as that species was understood by Hustedt (e.g. 1930), the two being separated by the more attenuated ends of *kuetzingioides*.

Were one to focus exclusively on the original description of *N. kuetzingioides* (Hustedt 1959), it would be easy to make a separation between this species and *N. agnita*. *Nitzschia agnita* was described by Hustedt (1957) as having extended narrow poles and capitate ends, whereas he explicitly stated of *N. kuetzingioides* (Hustedt 1959, p. 417) that the valves did *not* have capitate ends ("Schalen typisch lanzettlich mit deutlich geschnäbelten, spitz gerundeten, nicht kopfigen Enden") and this was clearly shown in his five illustrations of the species (Hustedt 1959, figs 25–29). In accordance with this, in their text description of *N. kuetzingioides*, Lange-Bertalot & Simonsen (1978) said that it had valves with "protracted ends with acute, non-capitate apices". However, in the specimens they illustrated from Hustedt's material from the Neusiedler See the apices are not acutely rounded as indicated by Hustedt but, in at least one case (Lange-Bertalot & Simonsen 1978, fig. 152), subcapitate or capitate. Later, in the much clearer micrographs by Simonsen (1987, figs 20–25) from the same Hustedt material, the apices are certainly capitate. It is difficult to account for these inconsistencies. Archibald (1983) suggested that *N. kuetzingioides* might "represent only the short specimens of *N. agnita*, distinguished merely on the lack of capitate apices" (this interpretation is consistent with the well-documented dogma that the morphology of pennate diatoms often simplifies during size reduction: Geitler 1932), but there is in fact full overlap between the size ranges recorded for the two species (Table 1). Or it could be argued that Lange-Bertalot & Simonsen (1978) and Simonsen (1987) made an error in choosing valves with capitate ends as representatives of *N. kuetzingioides*. However, against this, the list of 12 taxa of *Nitzschia* recorded in the Neusiedler See by Hustedt (11 species and one variety) includes no others with the same overall shape and dimensions as the specimens found and assigned to *N. kuetzingioides* by Simonsen and, in the same material studied by Lange-Bertalot and Simonsen, we found no better fit to Hustedt's description than they did (cf. Figs 8–12 and S4). Furthermore, Hustedt's original description of *N. kuetzingioides* was in fact

invalid, since from 1958 onwards it was obligatory to specify the types of new species (Turland *et al.* 2018, Art. 40.1) and this was not done. Consequently, we conclude that (1) Lange-Bertalot & Simonsen's (1978) choice of type was reasonable; (2) by typifying the species with slide 327/19b from "Neusiedler See, Grund 1", Lange-Bertalot & Simonsen satisfied the missing requirement for valid publication of *N. kuetzingioides*, which therefore dates from 1978, with authorship 'Hustedt *ex* Lange-Bertalot & Simonsen'; and (3) available descriptions of *N. kuetzingioides* valve morphology, including the original (invalid) description by Hustedt (1959), are misleading, since they explicitly exclude the valve morphology observable in most specimens in the type material, in which the ends are subcapitate or capitate.

Unlike *N. agnita*, *N. kuetzingioides* was first recorded in at least three samples and Hustedt (1959, p. 417) gave ranges for the length and fibula density, in contrast to the single values given for *N. agnita* (Table 1). Simonsen (1987, p. 461, pl. 688, figs 20–25) illustrated four specimens, all frustules, from one of the three samples and we examined material from this sample, E8145. Besides the sample from Neusiedl, Hustedt also listed two other samples as containing *N. kuetzingioides*, both also collected by Dr E. Peschek in May and June 1950, from Illmitz Bay and from where the Wulka river discharges into the Neusiedler See. *Nitzschia kuetzingioides* is not uncommon in sample E8145 from Neusiedl and we found both valves and frustules in LM and were able to study valve ultrastructure in SEM. Putting our observations together with those of Hustedt (1959) and Simonsen (1987), we can provide a fuller description of *N. kuetzingioides*:

The valves are narrowly lanceolate, having a smoothly changing curvature throughout (Figs 8–12, 27–29, S5): hence the central part of the valve lacks a linear section, as in *N. agnita*. The ends of the valves are drawn out and have very narrow, distinctly capitate apices (Figs 8–11, 27–29), except in the shortest (Fig. 12). Length 23–38 µm, width 3.3–3.6 µm,

with 12–17.3 fibulae in 10 µm (Table 1). Lange-Bertalot & Simonsen (1978) indicated lengths up to 43 µm and widths up to 4 µm, but we found no valves as wide as this. The central fibulae are not more widely separated and there is no central nodule. SEM revealed (3 measurements) a stria density of 49–51 in 10 µm, while Simonsen (1987) gave a value of 46–48 based on light microscopy (see Table 1, footnote 4). The average poroid spacing along the striae was 39.5, 42.4 and 45.1 in 10 µm in the three specimens found (n = 29, 28 and 29 respectively), thus overlapping with *N.* cf. *agnita*.

The internal valve ultrastructure agrees in all respects with that of *N. agnita*, including the tendency for the stria poroids to be more irregularly and more widely spaced than in *N.* cf. *agnita* (Figs 27–29, 34, 36: compare Figs 26, 33 of *N. agnita* and contrast Figs 23–25, 32 of *N.* cf. *agnita*). Externally, it seems that the narrower width of the valve near the poles in *N. kuetzingioides* than in *N.* cf. *agnita* is reflected in a reduced number of poroids per stria at any given distance from the pole (compare Figs 30, 31). The raphe slit was confirmed by SEM to be continuous across the centre of the valve (not illustrated). The raphe canal bears a single longitudinal row of poroids and the terminal fissure is short and bent to one side (Fig. 31), as in *N.* cf. *agnita* (Fig. 30).

No girdle bands were observed in specimens viewed by SEM. However, in LM, four partly disassembled frustules and thecae were observed (three are shown in Figs 53–55; the fourth can be focused interactively by viewing the Supplementary Video). Short bands were not seen in any of them; instead, robust full-length bands were present, thus separating *N. kuetzingioides* from *N.* cf. *agnita*, where the only full-length band is the extremely delicate band 5, which cannot on its own retain the shape of the valve (e.g. Fig. 48). In three of the specimens of *N. kuetzingioides*, the full-length element was attached to one pole but its arms spread apart at the other (Figs 53, 54, Supplementary Video), in one case like a ‘V-spring’ (Fig. 53) allowing direct comparison with an equivalent partial theca of *N.* cf. *agnita* (Fig.

51). In the remaining theca, the girdle had collapsed inwards, with a robust band traceable and unbroken for much more than half the length of the valve (Fig. 54). A further valve with half of a full-length robust girdle band is shown in Fig. S5, ee).

Other morphologically similar *Nitzschia* species

A number of other *Nitzschia* species have been compared with *N. agnita* by various authors and suggested to be synonymous or sufficiently similar for there to be confusion between them. Archibald (1983) synonymized his own *N. obligata* with *N. agnita*, but his original description of *N. obligata* (Archibald 1966) indicated a longer, more slender diatom (Table 1). The type slide is lost (Archibald 1983, p. 233). Archibald (1983) also compared *N. agnita* with Cholnoky's *N. irremissa*, but Cholnoky's description (1959, p. 57) indicates a much larger diatom (in both length and width: Table 1); besides, Cholnoky did not specify a type and so the name was not validly published and Archibald (1983) was unable to locate a slide that might be considered a type. A specimen attributed to *N. irremissa* photographed from a Cholnoky slide by Lange-Bertalot & Krammer (1987, pl. 38, fig. 23) shows a much smaller diatom (*c.* 26 × 2.7 µm, as measured from their photograph, with 18 fibulae in 10 µm) than Cholnoky described. In addition, the specimen found came from none of the six localities in Cape Province mentioned for the species by Cholnoky but instead from the Tugela river in KwaZulu-Natal.

A further species described by Cholnoky (1959), *N. capensis*, resembles *N.* cf. *agnita* in shape and valve dimensions but not in fibula density and most likely also in stria density (Table 1, footnote). Krammer & Lange-Bertalot (1988) gave *N. capensis* as a possible synonym of *N. agnita*, as did Sonneman *et al.* (1999). However, this is largely irrelevant because *N. capensis*, like *N. irremissa*, was not validly published because Cholnoky did not indicate a type. The illustration given for *N. capensis* by Lange-Bertalot & Krammer (1987,

fig. 24), like that of *N. irremissa*, is not from one of the sites in Cape Province listed by Cholnoky (1959) but instead from the Tugela river.

Lange-Bertalot & Simonsen (1978) regarded *N. kuetzingioides* and *N. agnita* as synonyms of *N. pumila* Hustedt, but the central section of the valve is clearly parallel-sided in *N. pumila*, contrasting with the smoothly curving profiles of the other two. By 1988, the idea of synonymy with *N. pumila* had been abandoned (Krammer & Lange-Bertalot 1988, pp 115–117). *Nitzschia pumila* is also narrower, even if its dimensions are extended beyond Hustedt's description to the metrics given by Krammer & Lange-Bertalot (Table 1).

DISCUSSION

Taxonomic conclusions

Comparisons of *N. agnita* and *N. kuetzingioides* are hampered by the rarity of *N. agnita* in the type material. However, the few specimens of *N. agnita* found in LM and SEM do not differ in any respect from the much more abundant specimens of *N. kuetzingioides* that are available (Figs 7–12, 26–29, 32, 33, 52–55). We therefore confirm Krammer & Lange-Bertalot's suggestion (Krammer & Lange-Bertalot 1988; see also Witkowski *et al.* 2000) that *N. kuetzingioides* is conspecific with *N. agnita*. *Nitzschia kuetzingioides* is therefore a redundant name, invalidly published by Hustedt (1959) and validated by Lange-Bertalot & Simonsen (1978), *N. agnita* having priority (from 1957). We reject synonymy with *N. obligata* on the basis of the evidence currently available, and with *N. pumila*, and note that further discussion of *N. irremissa* and *N. capensis* is pointless because neither was validly published.

Regarding *N.* cf. *agnita*, although valve shape and dimensions show no clear differences from *N. agnita* (now including also *N. kuetzingioides*; Table 1), girdle structure separates them, *Nitzschia* cf. *agnita* possessing short bands at all stages of the life cycle

observed (Figs 41–49, S3). Hints of other differences are given by the generally wider valves and broader range of valve widths in *N*. cf. *agnita* and the tendency for the stria poroids to be more regularly spaced, but confirmation of this requires better sampling of both species: the wider range and higher maximum for the valve width in *N*. cf. *agnita* could reflect extra variation as a result of growth in culture, although it could equally be a corollary of the girdle structure, the short bands allowing more flexibility than the longer open bands of *N. agnita*. We have not noticed equivalent variation in width in delicate *Nitzschia* species with full-length bands, such as *N. draveillensis* M. Coste & Ricard, and there is also no sign of it in *N. kuetzingioides* (Fig. S5).

Consequently, we describe *N.* cf. *agnita* as a new species, *N. captiva*:

Nitzschia captiva* D.G. Mann, Trobajo, Witkowski, Norico Yamada & J.J. Bolton, *sp. nov.

Figs 2–25, 30, 32, 35, 37, 38, 40–49, 52

DESCRIPTION: Valves linear-lanceolate to lanceolate, rather variable in outline (and sometimes even elliptical in the smallest valves), narrowing to pointed or slightly rostrate apices, 5–29 µm long (even shorter valves were found but were severely malformed) and 3.3–4.8 µm wide, with 13.7–16.8 fibulae in 10 µm (up to *c.* 19 in the smallest specimens); valve structure very fine, striae impossible to resolve in LM, 50–52 in 10 µm (higher in the smallest valves but rarely exceeding 55 in 10 µm). Striae uniseriate, containing tiny round poroids; each stria represented within the raphe canal by a single poroid. Raphe continuous at the centre, with short bent terminal fissures at the poles. Distal mantle weakly developed. Girdle comprising four robust short bands, each with two rows of slightly elongate poroids, and an extremely delicate fifth band that is full-length and open. Barcode sequence (*rbc*L): GenBank accession LC482715.

HOLOTYPE: E5899/1 (Royal Botanic Garden Edinburgh): clonal material of isolate IRTA-CC-152, isolated in November 2018 by micropipetting a single cell from a sample collected on 28 October 2018 from a tidal pool at Kommetjie, Cape Province, South Africa.

ETYMOLOGY: *captiva* refers to how the species was discovered (i.e. as the kleptoplastids of dinoflagellate *Durinskia capensis*).

Valve morphology does not permit reliable separation of *N. captiva* and *N. agnita*. From this perspective the two are 'cryptic', with a remarkable agreement in valve pattern and ultrastructure, except that the valves are rather wider in *N. captiva*. However, the two species can be separated reliably by their girdle structure – the first such example in diatoms.

Phylogenetic position

The striking similarity between *N. captiva* and *N. agnita* in valve outline, dimensions and ultrastructure might seem to suggest a close phylogenetic relationship. Unfortunately, no DNA sequence data are available for *N. agnita*. However, short bands are present in a variety of *Nitzschia* species that differ in valve morphology from *N. captiva* (Mann *et al.* 2021b), including some other finely striated species, namely *N. paleacea* (Grunow) Grunow and *Nitzschia* sp. BC0317, that are closely related to *N. captiva* according to the *rbc*L phylogeny (Fig. 1) but differ clearly from it in valve shape and pattern parameters (e.g. stria density). Hence either the girdle structure or the valve morphology or both must have been subject to convergent evolution. A further interesting point emerging from the *rbc*L gene tree (Fig. 1) is that *Nitzschia* clade 6B has provided the endosymbionts or kleptoplastids for a variety of different dinoflagellates belonging to the family Kryptoperidiniaceae, namely *Durinskia* cf. *baltica*, *D. capensis*, *D. oculata*, *D. baltica* (Levander) Carty & El.R. Cox, an undescribed *Durinskia* species, *Dinothrix rugata* (Maiko Tamura & T. Horiguchi) Norico Yamada & T. Horiguchi, *D. phymatodea* Norico Yamada & T. Horiguchi, *D. paradoxa* Pascher, *D. pseudoparadoxa* Norico Yamada & T. Horiguchi, *Kryptoperidinium triquetrum* (Ehrenberg) Tillmann, Gottschling, Elbrächter, Kusber & Hoppenrath and *Kryptoperidinium* sp. (Kretschmann *et al.* 2018; Yamada *et al.* 2020). Why this should be so is unclear. These dinoflagellates comprise by far the majority of the known dinoflagellate–diatom symbioses and yet the pattern of relationships among the diatoms involved implies that there have been

several or many independent origins of the endosymbionts (Yamada *et al.* 2017). It seems reasonable to suppose, therefore, that clade 6B diatoms possess characteristics that pre-adapt them to being used as temporary or permanent chloroplasts. Many clade 6B species are delicate, thin-walled and finely structured. Perhaps, therefore, they are 'easy prey' for grazers and have therefore provided more opportunities than other genera and families of diatoms for transitions from free-living diatoms to endosymbionts. Another possibility is that the ancestral dinotom used a member of *Nitzschia* clade 6B for its chloroplasts and gene transfer occurred from this diatom to the host dinoflagellate and species-specific metabolic connections were established (Horiguchi 2006). Subsequently, because the ancestral dinotoms had 'designed' their genes and metabolism for accommodating a member of *Nitzschia* clade 6B, the descendent dinotoms still showed a preference for this or some other *Nitzschia* clade 6B species for their chloroplasts. Decoding the dinotom genome would provide a clear answer about this possibility. In any case, it is noticeable that one of the few species of Bacillariaceae outside-clade 6B that has been used in the same way by dinoflagellates – the endosymbiont of *Durinskia kwazulunatalensis* – is likewise in a clade of small, finely structured diatoms (the genus *Simonsenia* Lange-Bertalot: Fig. 1).

Ecology and geographical distribution

In the taxonomic accounts given above we avoided using habitat as evidence for combining or separating *N. captiva* and morphologically similar species, to ensure that it was possible subsequently to comment on ecology without circularity (to avoid the argument 'it grows in different places so it must be a different species'). We note, however, that *N. captiva* was isolated from seawater, whereas *N. agnita* is known so far only from freshwaters and the Neusiedler See (recorded as *N. kuetzingioides*). In culture, however, *N. captiva* can be grown successfully at 16.6 PSU.

Nitzschia captiva is one of two 'essential' diatoms that are the preferred prey of the kleptoplastic dinoflagellate *Durinskia capensis*. Other diatom species can benefit *D. capensis* through their photosynthesis and/or digestion, but only the essential diatoms allow long-term survival and growth (Yamada *et al.*, unpublished observations).

Durinskia capensis, containing *N. captiva*, is known so far only from the Western Cape Province, South Africa (Pienaar *et al.* 2007; Yamada *et al.* 2017), where it occurs in tidal pools high on the shore. Subsequently, *N. captiva* was isolated from the same habitat. These sites form part of the cool-temperate west coast Benguela marine province, a globally significant marine upwelling system (Anderson *et al.* 2009). Similar sea temperature regimes occur from the Cape Peninsula (which includes the Kommetjie site) as far north as Lüderitz in southern Namibia. Monthly mean seawater temperatures are generally 12–16°C (somewhat higher in Saldanha Bay), although temperatures as low as 8°C can occur for a few days during major upwelling events (Smit *et al.* 2013). However, high-shore rock pool temperatures can reach 30°C at low spring tide on the west coast of the Cape Peninsula (Huggett & Griffiths 1986). *Durinskia capensis* forms very visible red-brown blooms at low tide in shallow rock pools in the extreme high intertidal. The pools are adjacent to large kelp forests of *Ecklonia maxima* (Osbeck) Papenfuss and *Laminaria pallida* Greville, and are sometimes filled with large amounts of drift seaweeds in various stages of decomposition. The bottoms of the rock pools usually have only small amounts of sand, and the pools appear to be flushed out regularly, presumably at spring tides. The Kommetjie site is particularly sheltered from large swells by the flat topography of the ledges of Table Mountain Sandstone, as well as their position in a small, sheltered embayment, known as 'the Kom'. The rock pools are seldom subject to dilution by rain in the summer (when the *Durinskia* blooms), as this is a winter rainfall region. The diatom species accompanying *N. captiva* (contained in *Durinskia* cells) included *Halamphora hybrida* (Grunow) Levkov, *Delphineis*

karstenii (Boden) G.A. Fryxell, *Amphora helenensis* Giffen and two unidentified biraphid species that, examined in SEM, showed similarity, in terms of valve striation and girdle construction, to *Parlibellus* E.J. Cox (e.g. Round *et al.* 1990) and *Sternimirus* Witkowski & Chunlian Li (Witkowski *et al.* 2016).

In contrast, the type habitat of *N. agnita* – the river Ochtum at Kattenesch, Germany – was freshwater and the diatom flora included a number of *Eunotia* and *Neidium* spp, as well as species characteristic of eutrophic conditions (Hustedt 1957). The Neusiedler See, where *N. agnita* was recorded as *N. kuetzingioides*, is a closed (endorheic) lake and does have elevated salinity, but only roughly a twentieth that of seawater, though from time to time (the last occasion was in the mid-nineteenth century) the lake dries out (Hustedt 1959; Padisàk & Dokulil 1994), presumably accompanied by hypersalinity in places. Bey & Ector (2013; our Table 1), who illustrate specimens that agree well with the concept of *N. agnita* developed here (though the figures lack girdle detail), characterized *N. agnita* as occurring in "milieux fortement minéralisés, voire saumâtres".

The geographical distributions of *N. agnita* and *N. captiva* are poorly known. Secure records of *N. agnita* come from Hustedt's original records of *N. agnita* and *N. kuetzingioides* in N Germany and E Austria respectively. In addition, there are illustrations that are certainly like *N. agnita*, as defined here, and may represent reliable records from the river Charpassonne at Panissières, France (Bey & Ector 2013; our Table 1), the Indian Ocean island of La Réunion (Gassiole *et al.* 2015, p. 225, pl. 18), India (Bharati *et al.* 2019, fig. 1I) and Australia (Sonneman *et al.* 1999; see our Table 1). However, since they are LM views of isolated valves or complete frustules and there is no information about valve ultrastructure, stria density or girdle, the records cannot be regarded as definitive. Clavero (2009) reported delicate *agnita*-like diatoms from hypersaline sites in Baja California (as '*Nitzschia* aff. *Nitzschia agnita*') and included SEM details of the valves, but no girdle band detail was

given. In at least some of her specimens (Clavero 2009, figs 5, 8, 11), the raphe appears to be less eccentric than in either *N. captiva* or *N. agnita*. Records of *agnita* from South Africa (e.g. Archibald 1983) are plausible but need further confirmation, given the many problems we have indicated concerning the taxonomy of similar South African *Nitzschia* species with attenuate ends. In other cases, published illustrations exclude identification as *N. agnita* (e.g. from China: Guo *et al.* 1999; Brazil: Bes & Torgan 2010; Argentina: Vouilloud & Leonardi 2001) because the dimensions are too small and/or the stria density is too low. A diatom identified as *N. agnita* was part of a marine phytoplankton community from the North Sea manipulated in chemostat experiments by Burson *et al.* (2018) but this record cannot be confirmed from the information given (no illustrations or description). A prominent member of the phytoplankton in a freshwater floodplain lake in Australia was likewise identified as *N. agnita* (Townsend 2006) but again confirmation is impossible. The records in the Global Biodiversity Information Facility (https://www.gbif.org/ searched 1 June 2022) are also unreliable, though many could potentially be checked.

Meanwhile, *N. captiva* is known from three marine coastal locations in Western Cape Province – Lamberts Bay, Saldanha Bay and Kommetjie. Uniquely for a diatom, its distribution is currently known, not from its frustules, but from its occurrence as kleptoplastids in specimens of *Durinskia capensis* collected between 1979 and 2018 (Pienaar *et al.* 2007; Yamada *et al.* 2017), though the earliest record did not characterize the kleptoplastids molecularly and therefore depends on whether *D. capensis* is always fastidious in preferring *N. captiva*. The only frustule-bearing cells known are those of IRTA-CC-152, isolated from Kommetjie.

REFERENCES

Anderson R.J., Bolton J.J. & Stegenga H. 2009. Using the biogeographical distribution and diversity of seaweed species to test the efficacy of marine protected areas in the warm-

temperate Agulhas Marine Province, South Africa. *Diversity and Distributions* 15: 1017–1027.

Archibald R.E.M. 1966. Some new and rare *Nitzschiae* (Diatomaceae) from the Vaal Dam catchment area (South Africa). *Portugaliae Acta Biologica, Séries B* 8: 227–238.

Archibald R.E.M. 1983. The diatoms of the Sundays and Great Fish Rivers in the Eastern Cape Province of South Africa. *Bibliotheca Diatomologica* 1: 1–362.

Bes D. & Torgan L.C. 2010. O gênero *Nitzschia* (Bacillariaceae) em ambientes lacustres na Planície Costeira do Rio Grande do Sul, Brasil. *Rodriguésia* 61: 359–382.

Bey M.-Y. & Ector L. 2013. *Atlas des diatomées des cours d'eau de la région Rhône-Alpes. Bacillariacées, Rhopalodiacées, Surirellacées*, vol. 6, pp 973–1182. Direction Régionale de l'Environnement, de l'Aménagement et du Logement Rhône-Alpes. ISBN 978-2-11-129817-0

Bharati R., Verma D. & Lavania S. 2019. Study on fresh water diatoms from different habitats of Patna, Bihar, India. *Journal of the Indian Botanical Society* 98: 157–165.

Burson A., Stomp M., Greenwell E., Grosse J. & Huisman J. 2018. Competition for nutrients and light: testing advances in resource competition with a natural phytoplankton community. *Ecology* 99: 1108–1118.

Chesnick J.M., Morden C.W. & Schmieg A.M. 1996. Identity of the endosymbiont of *Peridinium foliaceum* (Pyrrophyta): analysis of the *rbcLS* operon. *Journal of Phycology* 32: 850–857.

Cholnoky B.J. 1959. Neue und seltene Diatomeen aus Afrika IV. Diatomeen aus der Kaap-Provinz. *Österreichische Botanische Zeitschrift* 106: 1–69.

Clavero E. 2009. *Diatomees d'ambients hipersalins costaners: taxonomia. Distribució I empremtes en el registre sedimentari.* Institut d'Estudis Catalans, Barcelona. 432 pp.

Dodge J.D. 1971. A dinoflagellate with both a mesocaryotic and a eucaryotic nucleus. I. Fine structure of the nuclei. *Protoplasma* 73: 145–157.

Edler D., Klein J., Antonelli A. & Silvestro D. 2021. raxmlGUI 2.0: a graphical interface and toolkit for phylogenetic analyses using RAxML. *Methods in Ecology and Evolution* 12: 373–377.

Gassiole G., Boutry S., Picot A., Delmas F., Gwilherm J., Moreira S., Giraudel J.-L., Le Cohu R., Coste M. & Peres F. 2015. *Atlas des diatomées des eaux douces de l Île de La Réunion*. Office de l'eau Réunion, Île de La Réunion, France. 238 pp.

Geitler L. 1932. Der Formwechsel der pennaten Diatomeen. *Archiv für Protistenkunde* 78: 1–226.

Geitler L. 1975. Lebendbeobachtung der Chromatophorenteilung der Diatomee *Nitzschia*. *Plant Systematics and Evolution* 123: 145–152.

Gottschling M., Calasan A.Z, Kretschmann J. & Gu H.F. 2017. Two new generic names for dinophytes harbouring a diatom as an endosymbiont, *Blixaea* and *Unruhdinium* (Kryptoperidiniaceae, Peridiniales). *Phytotaxa* 306: 296–300.

Gottschling M., Tillmann U., Elbrächter M., Kusber W.-H. & Hoppenrath M. 2019. *Glenodinium triquetrum* Ehrenb. is a species not of *Heterocapsa* F. Stein but of *Kryptoperidinium* Er. Lindem. (Kryptoperidiniaceae, Peridiniales). *Phytotaxa* 391: 155–158.

Guo J., Liu S.-C. & Lin J.-H. 1999. Five newly-recorded species in the genus *Nitzschia* from China. *Acta Phytotaxonomica Sinica* 37: 526–528 [in Chinese].

Horiguchi T. 2006. Algae and their chloroplasts with particular reference to the dinoflagellates. *Paleontological Research* 10: 299–309.

Huggett J. & Griffiths C.L. 1986. Some relationships between elevation, physico-chemical variables and biota of intertidal rock pools. *Marine Ecology Progress Series* 29: 189–197.

Hustedt F. 1930. Bacillariophyta (Diatomeae). In: *Die Süsswasser-flora Mitteleuropas*, vol. 10, ed. 2 (Ed. by A. Pascher). G. Fischer, Jena, Germany. 466 pp.

Hustedt F. 1954. Die Diatomeenflora der Eifelmaare. *Archiv für Hydrobiologie* 48: 451–496.

Hustedt F. 1957. Die Diatomeenflora des Flußsystems der Weser im Gebiet der Hansestadt Bremen. Denkschrift über den heutigen ökologischen Zustand der Wasserstraßen im bremischen Staatsgebiet auf Grund der Kieselalgen-Flora mit Beziehung auf die Abwasserverhältnisse. *Abhandlungen herausgegeben vom Naturwissenschaftlichen Vereins zu Bremen* 34: 181–440.

Hustedt F. 1959. Die Diatomeenflora des Neusiedler Sees im österreichischen Burgenland. *Österreichische Botanische Zeitschrift* 106: 390–430.

Krammer K. & Lange-Bertalot H. 1988. Bacillariophyceae 2. Teil: Bacillariaceae, Epithemiaceae, Surirellaceae. In: *Süßwasserflora von Mitteleuropa* vol. 2 (2) (Ed. by H. Ettl, J. Gerloff, H. Heynig & D. Mollenhauer). Gustav Fischer, Stuttgart, Germany. 596 pp.

Kretschmann J., Čalasan A.Ž. & Gottschling M. 2018. Molecular phylogenetics of dinophytes harboring diatoms as endosymbionts (Kryptoperidiniaceae, Peridiniales), with evolutionary interpretations and a focus on the identity of *Durinskia oculata* from Prague. *Molecular Phylogenetics and Evolution* 118: 392–402.

Lange-Bertalot H. & Krammer K. 1987. Bacillariaceae, Epithemiaceae, Surirellaceae. Neue und wenig bekannte Taxa, neue Kombinationen und Synonyme sowie Bemerkungen und Ergänzungen zu den Naviculaceae. *Bibliotheca Diatomologica* 15: 1–289.

Lange-Bertalot H. & Simonsen R. 1978. A taxonomic revision of the *Nitzschiae lanceolatae* Grunow. 2. European and related extra-European fresh water and brackish water taxa. *Bacillaria* 1: 11–111.

Laslandes B., Spicuzza-Mocelin H., Ortiz-Lerin R., Garcia F., Ponton E., Cejudo-Figueiras C., Fayt G., Kermarrec L. & Coulon S. 2013. *Atlas des diatomées de l'Île de France*. DRIEE, Île de France, France. 734 pp.

Letunic I. & Bork P. 2021. Interactive Tree Of Life (iTOL) v5: an online tool for phylogenetic tree display and annotation. *Nucleic Acids Research* 49: W293–W296.

Lundholm N., Daugbjerg N & Moestrup O. 2002. Phylogeny of the Bacillariaceae with emphasis on the genus *Pseudo-nitzschia* (Bacillariophyceae) based on partial LSU rDNA.

European Journal of Phycology 37: 115–134. https://doi.org/10.1017/S096702620100347X

Mandelli E. 1968. Carotenoid pigments of the dinoflagellate *Glenodinium foliaceum* Stein. *Journal of Phycology* 4: 347–348.

Mann D.G. 1978. *Studies in the family Nitzschiaceae (Bacillariophyta)*. PhD thesis. University of Bristol, Bristol, UK. xxxiii + 386 pp, 146 pls. Available at https://rbg-web2.rbge.org.uk/algae/publications_mann_thesis.html.

Mann D.G., Trobajo R., Sato S., Li C., Witkowski A., Rimet F., Ashworth M.P., Hollands R.M. & Theriot E.C. 2021a. Ripe for reassessment: a synthesis of available molecular data for the speciose diatom family Bacillariaceae. *Molecular Phylogenetics and Evolutio*n 158: Article 106985. 10.1016/j.ympev.2020.106985.

Mann D.G., Wetzel C.E. & Trobajo R. 2021b. A new type of girdle band in Bacillariaceae. *Nova Hedwigia, Beiheft* 151: 141–159. 10.1127/nova-suppl/2021/141.

Mizuno M. 1987. Morphological variation of the attached diatom *Cocconeis scutellum* var. *scutellum* (Bacillariophyceae). *Journal of Phycology* 23: 591–597.

Padisàk J. & Dokulil M. 1994. Meroplankton dynamics in a saline, turbulent, turbid shallow lake (Neusiedlersee, Austria and Hungary). *Hydrobiologia* 289: 23–42.

Pienaar R.N., Sakai H. & Horiguchi T. 2007. Description of a new dinoflagellate with a diatom endosymbiont, *Durinskia capensis* sp. nov. (Peridiniales, Dinophyceae) from South Africa. *Journal of Plant Research* 120: 247–258. doi: 10.1007/s10265-006-0047-y.

Riley J.P. & Wilson T.R.S. 1967. The pigments of some marine phytoplankton species. *Journal of the Marine Biological Association of the United Kingdom* 47: 351–361.

Ross R., Cox E.J., Karayeva N.I., Mann D.G., Paddock T.B.B., Simonsen R. & Sims P.A. 1979. An amended terminology for the siliceous components of the diatom cell. *Nova Hedwigia, Beiheft* 64: 513–533.

Round F.E., Crawford R.M. & Mann D.G. 1990. *The Diatoms: biology and morphology of the genera*. Cambridge University Press, Cambridge, UK. 747 pp.

Simonsen R. 1987. *Atlas and catalogue of the diatom types of Friedrich Hustedt.* vols I–III. J. Cramer, Berlin & Stuttgart, Germany. 1741 pp, 772 pls.

Smit A.J., Roberts M., Anderson R.J., Dufois F., Dudley S.F.J., Bornman T.G., Olbers J. & Bolton J.J. 2013. A coastal seawater temperature dataset for biogeographical studies: large biases between in situ and remotely-sensed data sets around the coast of South Africa. *PLOS One* 8: Article e81944.

Sonneman J.A., Sincock A., Fluin J., Reid M., Newall P., Tibby J. & Gell P. 1999. *An illustrated guide to common stream diatom species from temperate Australia*. Cooperative Research Center for Freshwater Ecology, Thurgoona, Australia. 166 pp.

Stosch H.A. von 1975. An amended terminology of the diatom girdle. *Nova Hedwigia, Beiheft* 53: 1–35.

Tomas R.N. & Cox E.R. 1973. Observations on the symbiosis of *Peridinium balticum* and its intracellular alga. I. Ultrastructure. *Journal of Phycology* 9: 304–323.

Tomas R.N., Cox E.R. & Steidinger K.A. 1973. *Peridinium balticum* (Levander) Lemmermann, an unusual dinoflagellate with a mesocaryotic and an eucaryotic nucleus. *Journal of Phycology* 9: 91–98.

Townsend S.A. 2006. Hydraulic phases, persistent stratification, and phytoplankton in a tropical floodplain lake (Mary River, northern Australia). *Hydrobiologia* 556: 163–179.

Trobajo R., Mann D.G., Chepurnov V.A., Clavero E. & Cox E.J. 2006. Taxonomy, life cycle, and auxosporulation of *Nitzschia fonticola* (Bacillariophyta). *Journal of Phycology* 42: 1353–1372. 10.1111/j.1529-8817.2006.00291.x

Trobajo R. & Mann D.G. 2019. A rapid cleaning method for diatoms. *Diatom Research* 34: 115–124. 10.1080/0269249X.2019.1637785.

Turland N.J., Wiersema J.H., Barrie F.R., Greuter W., Hawksworth D.L., Herendeen P.S., Knapp S., Kusber W.-H., Li D.-Z., Marhold K. *et al.* [Eds] 2018. *International Code of Nomenclature for algae, fungi, and plants (Shenzhen Code) adopted by the Nineteenth International Botanical Congress Shenzhen, China, July 2017*. Koeltz Botanical Books,

Glashütten, Germany. xxxviii + 254 pp. [*Regnum Vegetabile* 159] DOI: https://doi.org/10.12705/Code.2018.

Vouilloud A.A. & Leonardi P.I. 2001. Bacillariophyceae de los Canales de Corfo (Río Colorado, Buenos Aires, Argentina). *Boletin de la Sociedad Argentina de Botanica* 36: 229–241.

Withers N. & Haxo F.T. 1975. Chlorophyll c_1 and c_2 and extraplastidic carotenoids in the dinoflagellate, *Peridinium foliaceum* Stein. *Plant Science Letters* 5: 7–15.

Witkowski A., Lange-Bertalot H. & Metzeltin D. 2000. Diatom flora of marine coasts. In: *Iconographia diatomologica,* vol. 7. *Diversity–taxonomy–identification* (Ed. by H. Lange-Bertalot), pp 1–925. A.R.G. Gantner, Ruggell, Liechtenstein.

Witkowski A., Li C., Zglobicka I., Yu S.-X., Ashworth M., Dąbek P., Qin S., Tang Ch., Krzywda M., Ruppel M. *et al*. 2016. Multigene assessment of biodiversity of diatom (Bacillariophyceae) assemblages from the littoral zone of the Bohai and Yellow Seas in Yantai Region of northeast China with some remarks on ubiquitous taxa. *Journal of Coastal Research* 74 (Special issue): 166–195.

Yamada N., Sym S.D. & Horiguchi T. 2017. Identification of highly divergent diatom-derived chloroplasts in dinoflagellates, including a description of *Durinskia kwazulunatalensis* sp. nov. (Peridiniales, Dinophyceae). *Molecular Biology and Evolution* 34: 1335–1351.

Yamada N., Bolton J.J., Trobajo R., Mann D.G., Dąbek P., Witkowski A., Onuma R., Horiguchi T. & Kroth P.G. 2019. Discovery of a kleptoplastic ‘dinotom’ dinoflagellate and the unique nuclear dynamics of converting kleptoplastids to permanent plastids. *Scientific Reports* 9: Article 10474. 10.1038/s41598-019-46852-y.

Yamada N., Sakai H., Onuma R., Kroth P.G. & Horiguchi T. 2020. Five non-motile dinotom dinoflagellates of the genus *Dinothrix*. *Frontiers in Plant Science* 11: Article 591050. doi: 10.3389/fpls.2020.591050.

TABLES

Table 1. Morphometric data for *Nitzschia captiva* (= "*N.* cf. *agnita*", IRTA-CC-152), *N. agnita* and *N. kuetzingioides*, and some further similar species. Where available, the measurements given are range (mean ± standard deviation); ND = no data.

Species	**Microscopy**	**Length[1] (µm)**	**Width[1] (µm)**	**Fibula density (# in 10 µm)**	**Stria density (# in 10 µm)**	**Material or source**
Nitzschia captiva (*n* = 14)	LM	27–28 (27.49 ± 0.35)	3.3–4.3 (3.89 ± 0.26)	13.7–16.4 (15.07 ± 0.83)	invisible	IRTA-CC-152 slide 54 R2 (IRTA slide collection)
Nitzschia captiva (*n* = 16)	LM	24–29 (25.74 ± 1.35)	3.4–4.8 (3.95 ± 0.38)	13.8–16.8 (15.15 ± 0.86)	invisible	RBGE slide E5899/1 of IRTA-CC-152
Nitzschia captiva (very numerous)	LM	9–13	3.7–4.3	13.5–19.0	invisible	IRTA slide 104 of IRTA-CC-152

Nitzschia captiva (*n* = 6)	SEM	25.6–28.0 (27.21 ± 0.85)	3.4–4.0 (3.75 ± 0.21	13.5–16.7 (15.12 ± 1.19)	50–52 (50.42 ± 0.92)	stub of E5899 material
Nitzschia captiva (*n* = 56)	SEM	5.6–19.7[2]	ND	ND	50–58[2]	stubs of E5912–E5916 material
Nitzschia agnita (*n* = 2)	LM	32–33 (32.58 ± 0.34)	3.3 (3.27 ± 0.02	15.5–15.6 (15.55 ± 0.07)	invisible	RBGE slides E5897/1, E5897/2 from Hustedt Collection material 10096
Nitzschia agnita (*n* = 1)	SEM	23.3	3.4	15.2	51	stub of Hustedt material 10096
Nitzschia agnita (*n* = 1?)	LM	*c.* 33	3.5	*c.* 18	invisible	Hustedt (1957) original description
Nitzschia agnita (*n* = 1)	LM	35	3.7	14.8 (16)[3]	invisible	measured from Simonsen (1997),

						pl. 661, fig. 5 (‘holotype’)
Nitzschia agnita (*n* = 1)	LM	35	3.7	15–18	invisible	Lange-Bertalot & Simonsen (1978), p. 16
Nitzschia kuetzingioides (*n* = 24)	LM	23–38 (31.12 ± 3.14)	3.3–3.6 (3.44 ± 0.08)	13.2–16.9 (14.46 ± 1.0)	invisible	RBGE slides E5898/1, E5898/3 from Hustedt collection material G8145
Nitzschia kuetzingioides (*n* = 3)	SEM	30–32 (30.80 ± 1.17)	3.3–3.4 (3.34 ± 0.04)	13.6–15.8 (15.07 ± 1.27)	49–51 (49.83 ± 1.04)	stub of Hustedt material G8145
Nitzschia kuetzingioides[4]	LM	31–35 (32.73 ± 1.56)	3.6	13.2–17.3 (15.04 ± 1.51)	46–48[5]	measured from Simonsen (1997), pl. 668, figs 20, 22,

						24, 25, or recorded by Simonsen, p. 461
Nitzschia kuetzingioides	LM	25–32	*c.* 3.5	12–16	> 40	Hustedt (1959, p. 417), original description
Nitzschia kuetzingioides	LM	25–43	3.5–4	12–16	invisible	Lange-Bertalot & Simonsen (1978)
Nitzschia agnita sensu Archibald	LM	26.7–39.2	2.9–3.5	14–20	invisible	Archibald (1966), p. 232, figs 356–358
Nitzschia agnita (syn. *kuetzingioides*)[6] (*n* = 9)	LM	31–34 (31.72 ± 1.07)	3.4–3.9 (3.64 ± 0.20)	12.0–16.2 (13.97 ± 1.35)	invisible	measured from Bey & Ector (2013), p. 1003, figs 1–9
Nitzschia cf. *agnita sensu* Laslandes *et al.* (*n* = 76)	LM	14.1–20.9	2.8–3.9	14–18	invisible	Laslandes *et al.* (2013)[7]
Nitzschia capensis, *nom. invalid.*	LM	23–35	3–4	9–10	>40[8]	Cholnoky (1959), p. 56, figs 284–287

Nitzschia irremissa, nom. invalid.	LM	45–65	3–5	*c.* 18	invisible	Cholnoky (1959), p. 57, figs 298–300
Nitzschia obligata	LM	45	2.5	14	invisible	Archibald (1966), p. 233, fig. 20
Nitzschia obligata	LM	30.5–47.5	3.0–3.2	12–16	invisible	Archibald (1983), p.233
Nitzschia pumila	LM	30–35	2.5	16–18	invisible	Hustedt (1954, p. 480) original description
Nitzschia pumila	LM	30–37	2.5–3	14–18	invisible	Krammer & Lange-Bertalot (1988), p. 115

[1] Length measurements recorded in LM were rounded off to the nearest µm; widths were rounded off to the nearest 0.1 µm.

[2] These measurements were from five separate cultures: for further detail, see Table S1.

[3] The value of 14.8 in 10 µm was made over 10 µm in the centre and is comparable to the LM measurements for other material; measurement over 20 µm (hence extending closer to the apices) gave 16 in 10 µm. No part of the valve gave a value as high as 18 in 10 µm over distances of 10 µm.

[4] The specimens illustrated by Simonsen (1997) were all frustules or even (*op. cit.*, fig. 20) a recently divided cell with two conjoined frustules. In some cases it is therefore impossible to measure length, width or fibula density. The values we give are based on $n = 4$ (length), 2 (width) and 8 (fibula density)

[5] These stria densities were given by Simonsen (1997, p. 461), in a remarkable feat of light microscopy. We attempted to recount the stria densities from his photographs but this was extremely difficult. It seemed, however, that the lower value given by Simonsen, 46 in 10 µm, might be too low since there were apparently 48 in 10 µm in the frustule in his plate 688, fig. 23; in fig. 21 they were uncountable over a sufficient distance.

[6] Bey & Ector (2013) regarded *N. agnita* and *N. kuetzingioides* as synonyms. Of the nine specimens illustrated by Bey & Ector, two (figs 2 and 3) were frustules: from their fig. 2 we derived a single length measurement and a single width measurement but two fibula densities, one for each valve; in fig. 3 we again derived a single length measurement and two fibula densities, but the valve width could not be determined. No length or width measurement could be obtained from fig. 6 because the valve was not lying flat. Consequently, the averages and standard deviations given here for valve parameters are based on 7 (length), 7 (width) and 11 (fibula density) measurements.

[7] Laslandes *et al.* (2013) compared their diatom, from the La Marne river at Torcy, France, with *N. agnita* as understood by Krammer & Lange-Bertalot (1988), in which *N. agnita* was taken to be synonymous with *N. kuetzingioides* and regarded as part of a species complex ('Sippenkreise') also containing *N. aequorea*. In this treatment, *aequorea* and *agnita* 'Sippen' were separated according to the stria density – 30–35 in 10 µm in *aequorea*, over 35 in *agnita*. Laslandes *et al.*'s specimens resemble *N. agnita* and *N. kuetzingioides* in shape, width and fibula density, but there is a discrepancy between the length ranges recorded (14– 21 versus 23–43 for confirmed *kuetzingioides*): until this is bridged and/or other evidence is available (e.g. gene sequences), the shorter specimens cannot be assigned confidently to *N. agnita*.

[8] Cholnoky specifically stated that he could, by specially mounting specimens in methyl iodide, resolve the striae in *N. capensis*, though he did not count them. However, methyl iodide has more or less the same refractive index (1.74) as the currently used mountant Naphrax and we judge that it is very unlikely that Cholnoky would have been able to resolve striae with a density of more than 45 in 10 µm, even with an immersed condenser.

LEGENDS FOR FIGURES

Fig. 1. Phylogenetic tree of Bacillariaceae, based on a maximum-likelihood analysis of available *rbc*L sequences (until May 2022, reduced to unique sequences) and rooted with Eunotiales. Most of the main clades identified by Mann *et al.* (2021) have been collapsed to aid clarity. Clade 6B, to which *N. captiva* belongs, occupies the sector from 5 o'clock to 10 o'clock in the diagram and is sister to clade 6A. As well as free-living diatoms, clade B includes several diatom-derived dinoflagellate endosymbionts and kleptoplastids (in blue, bold), including the *Durinskia capensis* kleptoplastids derived from *N. capensis*. However, the diatom-derived endosymbionts of *D. kwazulunatalensis* are in the *Simonsenia* clade.

Figs 2–22. *Nitzschia captiva sp. nov.* (*N.* cf. *agnita* in previous publications), *N. agnita* and *N. kuetzingioides*, LM. Scale bars = 5 µm (for valve images, see Fig. 6, for living cells, see Fig. 20).

Figs 2–6. *Nitzschia captiva* valves. Note the rostrate ends and the variation in valve outline, from those with linear central sections (Figs 2, 3) to those with a more gradual curvature of the sides (Fig. 4).

Fig. 7. *Nitzschia agnita* frustule from type material, focused on one of the valves. Note the ± gradual curvature of the sides and the extremely narrow, slightly capitate apices.

Figs 8–12. *Nitzschia kuetzingioides* valves, type material: a range of lengths from the longest to the shortest found. The valve outline corresponds to that in *N. agnita* (cf. Fig. 7), with very regular diminution of the width from the centre outwards to close to the ends and the extremely narrow, slightly capitate apices.

Figs 13–16. *Nitzschia captiva*: living cells (in valve view) after months in culture: the valve length has reduced considerably and the valve outline is simpler, with very slightly rostrate or simply rounded apices. Cells contain a central nucleus (Fig. 15, arrow) and two chloroplasts in a fore-and-aft arrangement, each with a single pyrenoid (Fig. 13, arrow).

Figs 17–22. *Nitzschia captiva*: living cells in girdle view, in early (Fig. 17) and late interphase (Figs 18, 19), and recently divided. Note the volutin granules (arrows) at the polar ends of the chloroplasts. Fig. 22 shows a teratological cell with a bent profile

Figs 23–29. Internal views of valves, SEM, zero tilt. Scale bar = 10 µm.

Figs 23–25. *Nitzschia captiva sp. nov*.

Fig. 26. *Nitzschia agnita*.

Figs 27–29. *Nitzschia kuetzingioides*. Note the narrower, more capitate poles of *N. agnita* and *N. kuetzingioides*.

Figs 30–40. Ultrastructure of valves, SEM, zero tilt (Figs 30–34, 40) or 25° (Figs 35–39).

Figs 30, 31. External views of the apices of *N. captiva sp. nov.* and *N. kuetzingioides*, respectively, at the same scale. Note the narrower apices of *N. kuetzingioides*. Both species have a single row of poroids within the raphe canal (arrows). Scale bars = 500 nm.

Figs 32–34. Comparable parts of the valve interior in *N. captiva sp. nov.*, *N. agnita* and *N. kuetzingioides*, respectively: note the wider spacing of the poroids along the striae in *N. agnita* and *N. kuetzingioides*, compared to *N. captiva*. The fibulae appear more rib-like in Fig. 32 of *N. captiva* but this feature is not consistent in the species (cf. Figs 23, 24). Note the longitudinal (apical) ridges connecting the fibula bases (arrows in Figs 32, 34). Scale bars = 500 nm.

Fig. 35. *Nitzschia captiva sp. nov.*, part of the valve interior, showing the very narrow plain margin of the vale distal to the raphe, and the presence of a single row of poroids between the fibula bases and the raphe. Scale bar = 500 nm.

Fig. 36. *Nitzschia kuetzingioides* interior: the structure is very similar to *N. captiva* (Fig. 35), except the stronger silicification and upturn of the distal mantle. Scale bar = 500 nm.

Fig. 37. *Nitzschia captiva sp. nov.*, internal view. Scale bar = 1 µm.

Fig. 38. *Nitzschia captiva sp. nov.*, disassembled frustule, allowing comparison of the interior and exterior: the poroids appear deeper and better defined from the interior, reflecting the positions of the hymenes, which lie closer to the external surface. Scale bar = 1 µm.

Fig. 39. Exterior of *N. kuetzingioides*. In this specimen the transapical ribs (virgae) appear to project externally more than in *N. captiva sp. nov.* but the structure is otherwise very similar. Scale bar = 500 nm.

Fig. 40. Whole valve of *N. captiva sp. nov.*, exterior view. The raphe slit is continuous from pole to pole. Scale bar = 1 µm.

Figs 41–49. Girdle structure in *Nitzschia captiva sp. nov.*, SEM (except Figs 41, 42).

Figs 41, 42. Disassembled thecae and girdle bands, LM. Note that the shorter lengths of the principal girdle bands (bands 1–4) are clearly visible. Scale bars = 5 µm.

Fig. 43. Valve and band 1 (arrow), tilted 25°. Scale bar = 5 µm.

Fig. 44. Almost intact frustule, zero tilt. Note the central 'splits' in the girdle, marking the ends of the short bands. Scale bar = 1 µm.

Fig. 45. Disassembled frustule from a recently divided cell. The epivalve (below) is complete, whereas the hypovalve is in an early stage of formation. Between the two are the short bands (which are almost broken at their centres, i.e. at the poles of the cell). Scale bar = 1 µm.

Fig. 46. Detail of the frustule in Fig. 44, showing the unequally tapered ends of the short bands. Bands 1–4 are numbered; band 5 is arrowed. Scale bar = 1 µm.

Fig. 47. Bands 1 (white arrows) and 3 (black arrows) of a cingulum: band 1 is wider, with slightly more widely spaced poroids. A fragment of band 5 is also visible (arrowhead). Scale bar = 1 µm.

Fig. 48. The extremely narrow, delicate band 5 of a cingulum, still mostly attached to band 4 (right). Scale bar = 1 µm.

Fig. 49. End of the frustule of a dividing cell. Note the closed ends of the short bands (arrowhead). A very early stage of valve formation is visible in the centre, in which the fibulae (present on only one side of the raphe) are still only stubby outgrowths borne from a few of the transapical ribs. Scale bar = 1 µm.

Figs 50–55. Separation of *N. captiva sp. nov.* from *N. agnita* and *N. kuetzingioides* in LM. In *N. captiva* disrupted frustules display irregular striations and hiatuses near the centre, reflecting the separation of the short bands (Fig. 50, arrowheads; compare Fig. 44). When disassembly is more extreme, a band can remain associated with its valve at the apex but spreads out elsewhere like a V-spring (Fig. 51, arrowheads), showing that it is much shorter than the valve it is attached to. In contrast, in *N. agnita* (Fig. 52) and *N. kuetzingioides* (Figs 53–55), the 'V-springs' (arrowheads) are as long as the valve, indicating that the advalvar bands are not short bands but normal open bands, like those in most pennate diatoms. Fig. 52. One of the two frustules found of *N. agnita* (cf. a second focus in Fig. 7): a displaced girdle

band (arrowheads) can be seen crossing the space inside the frustule, in such a way (its continuous curvature: contrast Fig. 50) that it must be a full-length open band. Figs 53–55. Three frustules of *N. kuetzingioides*, also showing full-length open bands (arrowheads), both within the frustule (Fig. 55) and projecting away from it (Figs 53, 54). Scale bar = 5 µm.

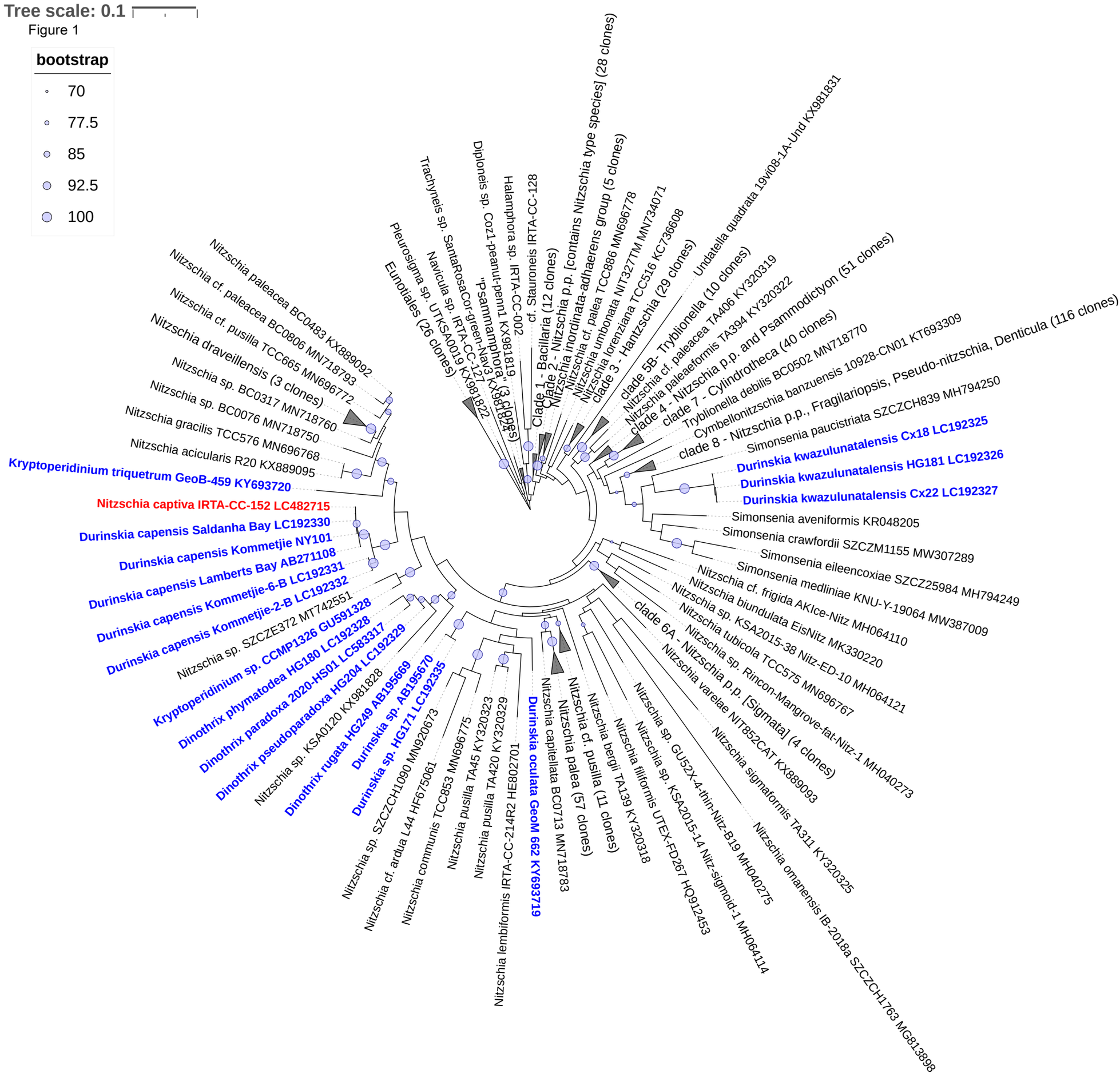
Tree scale: 0.1
Figure 1
bootstrap
70
77.5
85
92.5
100
Undatella quadrata 19vi08-1A-Und KX981831
clade 5B- Tryblionella (10 clones)
Nitzschia cf. paleacea TA406 KY320319
Nitzschia paleaeformis TA394 KY320322
clade 4 - Nitzschia p.p. and Psammodictyon (51 clones)
clade 7 - Cylindrotheca (40 clones)
Tryblionella debilis BC0502 MN718770
Cymbellonitzschia banzuensis 10928-CN01 KT693309
Simonsenia p.p., Fragilariopsis, Pseudo-nitzschia, Denticula (116 clones)
Simonsenia paucistriata SZCZCH839 MH794250
clade 8 - Nitzschia p.p., Fragilariopsis, Pseudo-nitzschia, Denticula (116 clones)
Durinskia kwazulunatalensis Cx18 LC192325
Durinskia kwazulunatalensis HG181 LC192326
Durinskia kwazulunatalensis Cx22 LC192327
Simonsenia aveniformis KR048205
Simonsenia crawfordii SZCZM1155 MW307289
Simonsenia eileencoxiae SZCZ25984 MH794249
Simonsenia medliniae KNU-Y-19064 MW387009
Nitzschia cf. frigida AKIce-Nitz MH064110
Nitzschia biundulata EisNitz MK330220
Nitzschia sp. KSA2015-38 Nitz-ED-10 MH064121
Nitzschia tubicola TCC575 MN696767
clade 6A - Nitzschia p.p. [Sigmata] (4 clones)
Nitzschia sp. Rincon-Mangrove-fat-Nitz-1 MH040273
Nitzschia varelae NIT852CAT KX889093
Nitzschia sigmaformis TA311 KY320325
Nitzschia omanensis IB-2018a SZCZCH1763 MG813898
Nitzschia sp. GU52X-4-thin-Nitz-B19 MH040275
Nitzschia sp. KSA2015-14 Nitz-sigmoid-1 MH064114
Nitzschia filiformis UTEX-FD267 HQ912453
Nitzschia bergii TA139 KY320318
Nitzschia cf. pusilla (11 clones)
Nitzschia palea (57 clones)
Nitzschia capitellata BC0713 MN718783
Durinskia oculata GeoM 662 KY693719
Nitzschia lembiformis IRTA-CC-214R2 HE802701
Nitzschia pusilla TA420 KY320329
Nitzschia pusilla TA45 KY320323
Nitzschia communis TCC853 MN696775
Nitzschia cf. ardua L44 HF675061
Nitzschia sp. SZCZCH1090 MN920673
Durinskia sp. HG171 LC192335
Durinskia sp. AB195669 AB195670
Dinothrix rugata HG249 AB195669
Dinothrix paradoxa HG204 LC192329
Dinothrix pseudoparadoxa 2020-HS01 LC583317
Dinothrix phymatodea HG180 LC192328
Kryptoperidinium sp. CCMP1326 GU591328
Nitzschia sp. KSA0120 KX981828
Nitzschia sp. SZCZE372 MT742551
Durinskia capensis Kommetjie-2-B LC192332
Durinskia capensis Kommetjie-6-B LC192331
Durinskia capensis Lamberts Bay AB271108
Durinskia capensis Kommetjie NY101
Durinskia capensis Saldanha Bay LC192330
Nitzschia captiva IRTA-CC-152 LC482715
Kryptoperidinium triquetrum GeoB-459 KY693720
Nitzschia acicularis R20 KX889095
Nitzschia gracilis TCC576 MN696768
Nitzschia sp. BC0076 MN718750
Nitzschia sp. BC0317 MN718760
Nitzschia draveillensis (3 clones)
Nitzschia cf. pusilla TCC665 MN696772
Nitzschia cf. paleacea BC0806 MN718793
Nitzschia paleacea BC0483 KX889092
Eunotiales (26 clones)
Pleurosigma sp. UTKSA0019 KX981822
Navicula sp. IRTA-CC-127
Trachyneis sp. SantaRosaCor-green-Nav3 KX981819
"Psammamphora" (3 clones)
Diploneis sp. Co21-peanut-peanut1 KX981824
Halamphora sp. IRTA-CC-002
cf. Stauroneis IRTA-CC-128
Clade 1 - Bacillaria (12 clones)
Clade 2 - Nitzschia p.p. [contains Nitzschia type species] (28 clones)
Nitzschia inordinata-adhaerens group (5 clones)
Nitzschia cf. palea TCC886 MN696778
Nitzschia umbonata NIT327TM MN734071
Nitzschia lorenziana TCC516 KC736608
clade 3 - Hantzschia (29 clones)

Figures 2 to 22

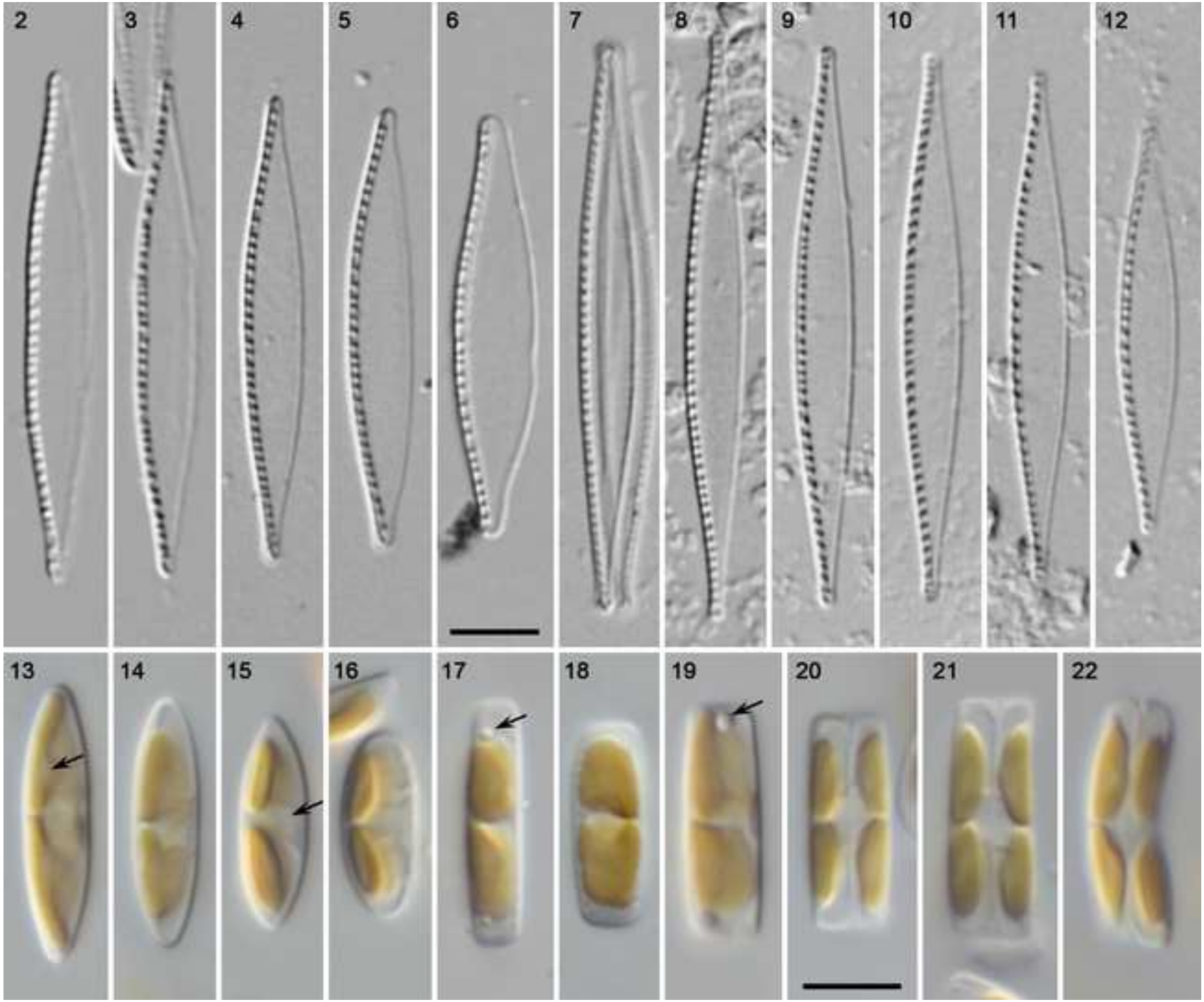

Figures 23 to 29

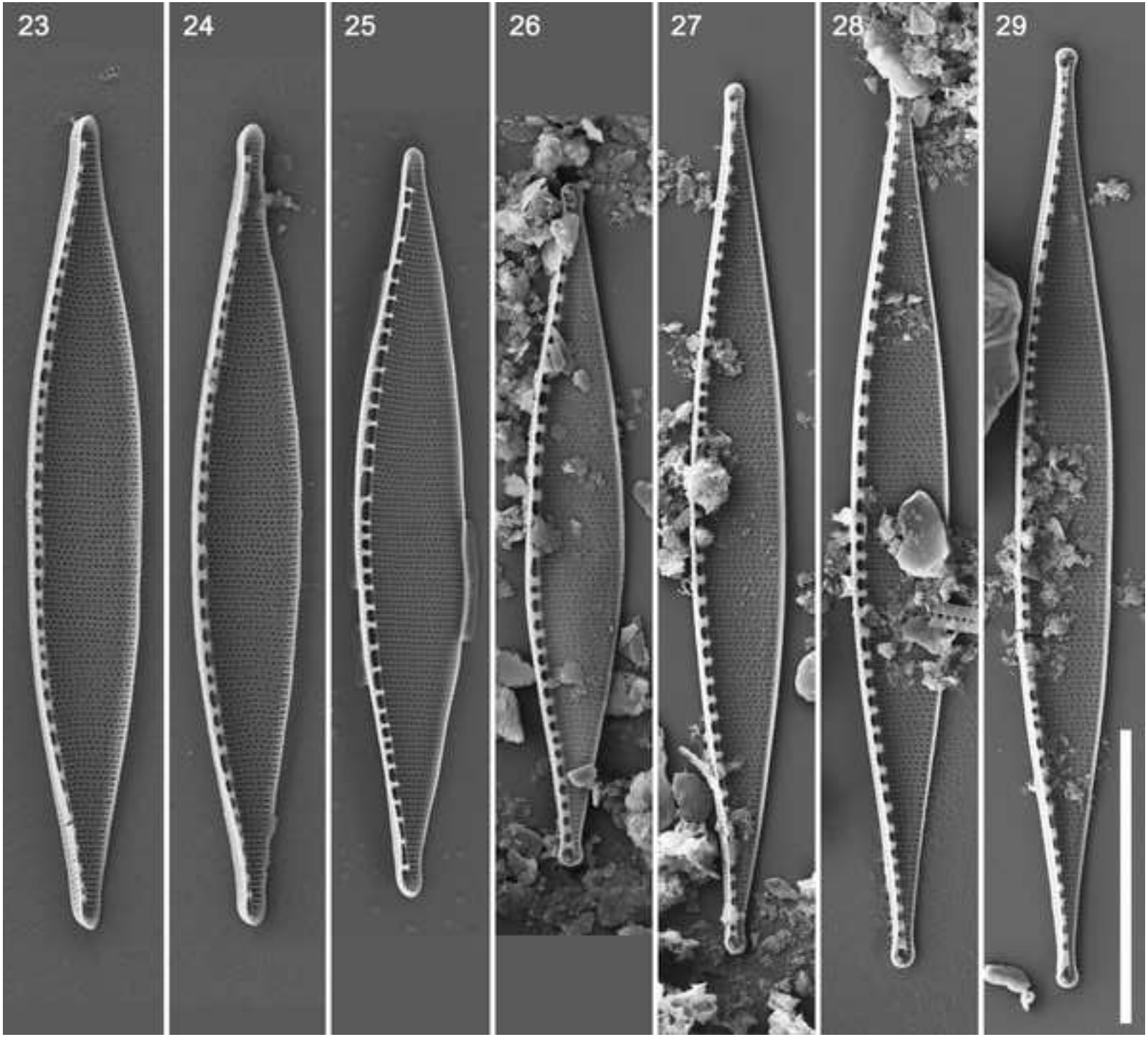

Figures 30 to 40

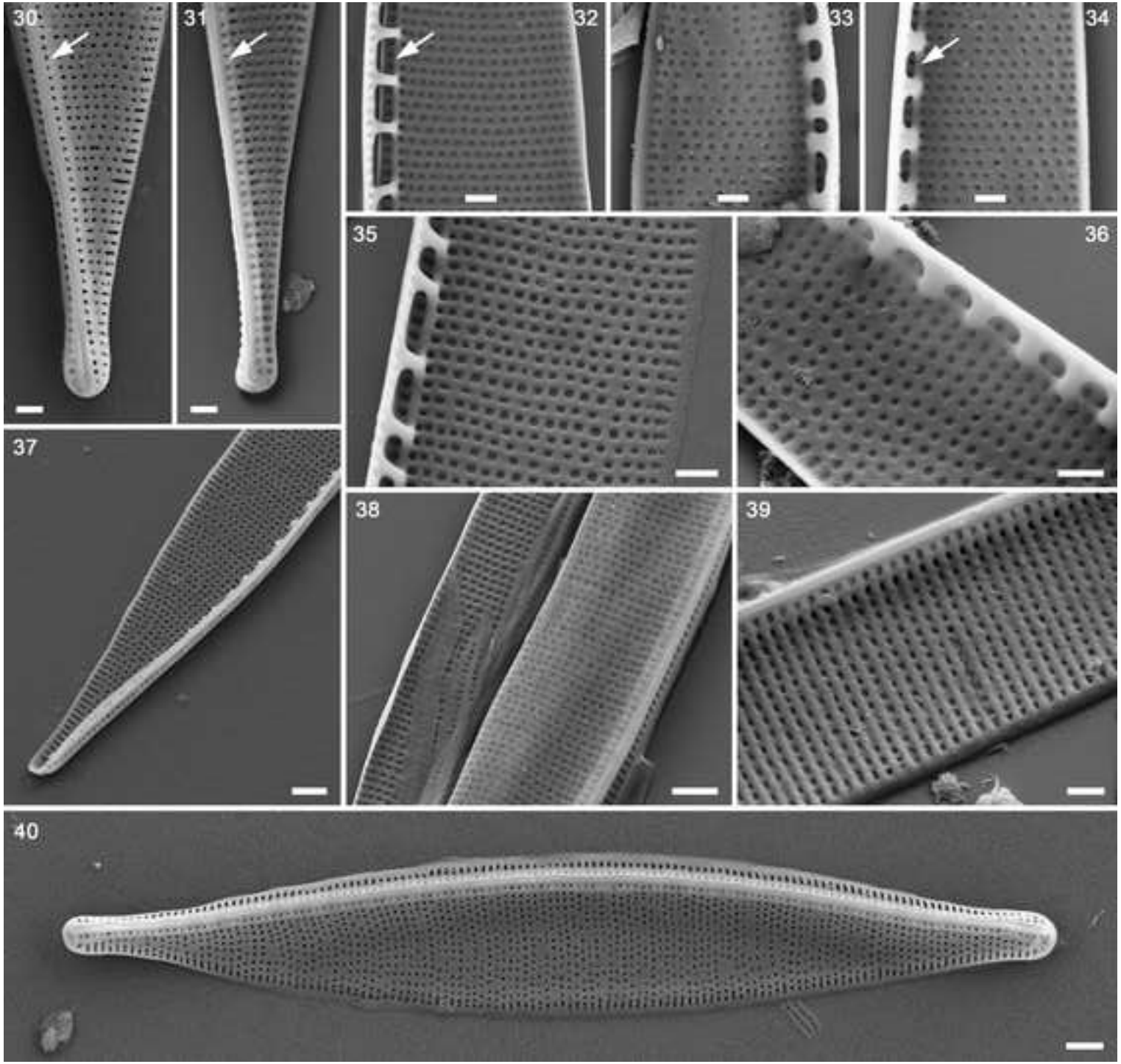

Figures 41 to 49

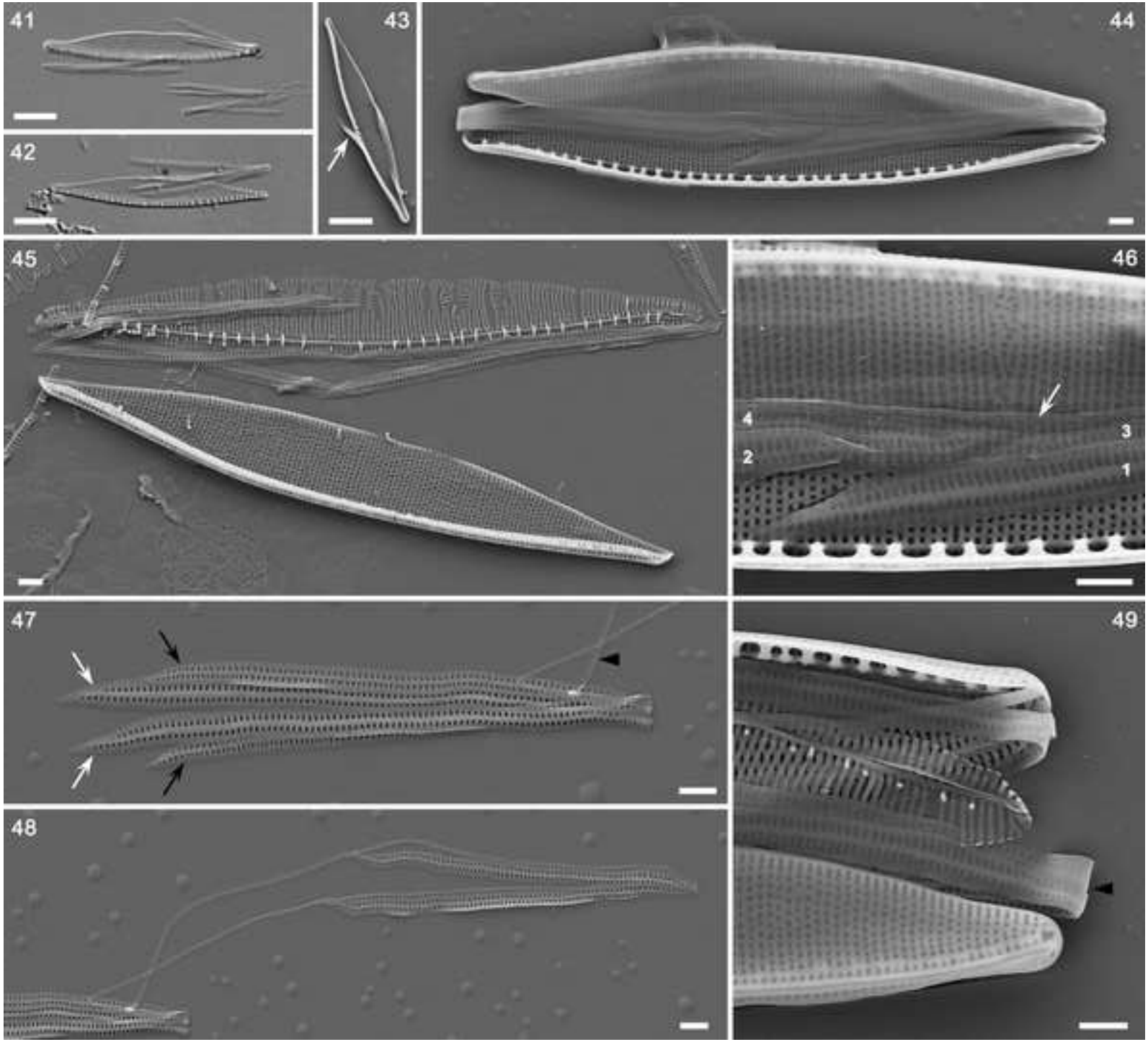

Figures 50 to 55